Supplement of Atmos. Meas. Tech., 9, 3477–3490, 2016
http://www.atmos-meas-tech.net/9/3477/2016/
doi:10.5194/amt-9-3477-2016-supplement

Atmospheric Measurement Techniques
Open Access
EGU

Supplement of

A new approach for retrieving the UV–vis optical properties of ambient aerosols

Nir Bluvshtein et al.

Correspondence to: Yinon Rudich (yinon.rudich@weizmann.ac.il)

Correction of nephelometer data due to hygroscopic growth

Hygroscopic growth of aerosols due to elevated relative humidity (RH) may significantly change the particle size and composition. As a result, the aerosol–radiation interactions may also change significantly.

Several studies have set out to model and predict the scattering enhancement factor ($f(RH)_\lambda$) using information about the dry aerosols chemical composition, optical properties and size (Nessler et al., 2005a; Zieger et al., 2013). Their objective was to correct optical measurements of dry aerosols to represent ambient conditions. The purpose of this section is to describe the correction procedure of ambient measurements of the AirPhoton IN100 integrating nephelometer to represent dry conditions (RH < 20%).

Snider et al., (2015) suggested to correct nephelometer ambient measurements for increased scattering due to growth of humidified particles at RH of up to 80% by the particles volumetric growth factor (VGF) with assumption regarding the hygroscopicity parameter (κ). While this correction accounts, to some extent, for the increased scattering due to the increased size, it does not take into account the decrease in effective RI of the particles due to water uptake.

The scattering enhancement factor is the key parameter used to describe the change in aerosols light scattering due to hygroscopic growth and is defined by:

$$f(RH)_\lambda = \frac{\alpha_{sca\_wet}(RH)_\lambda}{\alpha_{sca\_dry}(\lambda)} \quad (1)$$

where λ is the wavelength, $\alpha_{sca\_wet}(RH)_\lambda$ is the scattering coefficient of the humidified aerosols and $\alpha_{sca\_dry}(\lambda)$ is the scattering coefficient of the dry aerosols. We note that the scattering enhancement factor is also dependent on κ, complex RI ($m = n+ik$) and size distribution ($dN(D_P)$) but is termed $f(RH)_\lambda$ for simplicity.

To correct the nephelometer measurements done in ambient conditions we use measurements and simulations based on predictions from Mie theory to calculate $f(RH)_\lambda$ at the three wavelengths of the nephelometer; i.e., λ = 637, 525, and 457 nm.

We first correct the ambient nephelometer measurements at 637 nm. For this, we use the extrapolation of the BBCES extinction measurement described in the main text together with the assumption of negligible absorption at λ = 637 nm to calculate $f(RH)_{637nm}$. Then we use $f(RH)_{637nm}$ at each measurement together with parameterization of the ratio of $f(RH)_{637nm}$ to $f(RH)_{525nm}$ ($f(RH)_{637nm}$ / $f(RH)_{525nm}$) and the ratio of $f(RH)_{637nm}$ to $f(RH)_{457nm}$ ($f(RH)_{637nm}$ / $f(RH)_{457nm}$) based on Mie theory simulations to correct the ambient nephelometer measurements at the other two wavelengths of the IN; i.e., λ = 525, and 457 nm. We chose to parameterize the $f(RH)_{637nm}$ / $f(RH)_\lambda$ rather than simply $f(RH)_\lambda$ because the latter is a stronger function of aerosol size, κ and complex RI. In that respect, $f(RH)_{637nm}$ serves to restrict the scattering correction at 457 and 525 nm.

For the calculation of $f(RH)_{637nm}$ (termed $f(RH)_{637nm\_calc}$) we assumed that the absorption at λ = 637 nm is negligible. In other words, the dry scattering coefficient (α_{sca_dry}) is equal to the dry extinction coefficient (α_{ext_637nm}) extrapolated from the BBCES extinction measurements. The $f(RH)_{637nm\_calc}$ can then be calculated as:

$$f(RH)_{637nm\_calc} = \frac{\alpha_{sca\_wet\_637nm(RH)}}{\alpha_{ext\_637nm}} \quad (2)$$

To correct the $\alpha_{sca\_wet}(RH)_\lambda$ at the other two wavelength (457 and 525 nm) we used a Mie theory algorithm (Bohren and Huffman, 1983) to simulated $f(RH)_{637nm}$ / $f(RH)_{457nm}$ and $f(RH)_{637nm}$ / $f(RH)_{525nm}$ for a wide range of parameters. For these simulations we assumed: (1) that the dry particles population is composed of spherical and homogenously mixed particles such that there optical properties can be represented with an effective complex RI as defined in the main text; (2) the dry particle volume and the water volume composing the wet particle are additive; (3) the Kelvin effect is negligible; (4) the light absorption at 637 nm is negligible; and (4) the complex RI of the wet particles can be calculated using the volume weighted mixing rule (Nessler et al., 2005b; Flores et al., 2012; Zieger et al., 2013), where the real part of the humidified particles ($n_{wet}(\lambda)$) is calculated as:

$$n_{wet}(\lambda) = \frac{n_{dry}(\lambda) + n_{water}(\lambda) * (VGF(RH,\lambda) - 1)}{VGF(RH,\lambda)} \quad (3)$$

and the imaginary part of the humidified particle ($k_{wet}(\lambda)$) as:

$$k_{wet}(\lambda) = \frac{k_{dry}(\lambda)}{VGF(RH,\lambda)} \quad (4)$$

where $n(\lambda)$ and $k(\lambda)$ are the real and imaginary parts of the complex RI of the dry or the hydrated aerosols and $n_{water}(\lambda)$ is the refractive index of water.

Besides these four assumptions, we take into account the particle diameter growth factor (DGF = $VGF^{1/3}$), defined as:

$$DGF(RH) = \frac{D_{wet}(RH)}{D_{dry}} \quad (5)$$

where D_{wet} is the diameter of the humidified particles at ambient RH and D_{dry} is the diameter of the dry particle. The particle DGF is strongly related to its chemical composition, i.e. its hygroscopicity. And can be defined by:

$$DGF(a_w) = \left(1 + \kappa \frac{a_w}{1 - a_w}\right)^{\frac{1}{3}} \quad (6)$$

where the hygroscopicity parameter (κ) is a scaling variable for the dependence of the particle volumetric water content on water activity (a_w) (Petters and Kreidenweis, 2007). κ can range from 0 for non-hygroscopic particles such as soot, mineral dust and aerosols with high organic content, to above 1 for highly hygroscopic particles such as sea salt. a_w can be replaced by RH in equation 6 since we assume that the Kelvin effect is negligible.

To simulate the suburban aerosol population in our sampling site and to parameterize $f(RH)_{637nm}$ / $f(RH)_{525nm}$ and $f(RH)_{637nm}$ / $f(RH)_{457nm}$ the following parameters were used: (a) we used three different size distribution; two single mode log-normal distributions, one with a mode at 80 nm and the other at 100 nm. Both distributions had a geometric standard deviation of 1.33. The third size distributions used was a typical tri-modal urban size distribution following Seinfeld and Pandis, (2006); (b) we varied κ from 0.1 to 0.5 in steps of 0.2; (c) we varied the complex RI at λ = 457 nm from 1.4 to 1.7 in steps of 0.03 for the real part (Moise et al., 2015) and from 0 to 0.18 in steps of 0.02 for the imaginary part; (d) n at 525 nm and at 637 nm were determined as n_{457nm}-$C \cdot (\lambda_i - 457)$ where $10^{-4} \leq C \leq 50^{-4}$ (e.g. if n_{457nm}=1.550, $1.516 \leq n_{525nm} \leq 1.543$ and $1.460 \leq n_{637nm}$

≤ 1.532) and maintaining that $n_{637nm} < n_{525nm}$ (Moise et al., 2015). (e) k at 525 nm was determined as $C' \cdot k_{457nm}$ where $0.5 \leq C' \leq 0.05$ and k at 637 nm is zero (Moise et al., 2015).

The $f(RH)_{637nm} / f(RH)_{\lambda}$ from all the simulations were averaged and empirical curves were fitted to the average values and to the lower and upper limits (Fig. S1).

$$\frac{f(RH)_{637nm}}{f(RH)_{457nm_{para}}} = 9.929 \cdot 10^{-1} \cdot (1 - RH)^{-6.213 \cdot 10^{-2}} \quad (9)$$

$$\frac{f(RH)_{637nm}}{f(RH)_{525nm_{para}}} = 9.941 \cdot 10^{-1} \cdot (1 - RH)^{-5.390 \cdot 10^{-2}} \quad (10)$$

with upper limits of:

$$\frac{f(RH)_{637nm}}{f(RH)_{457nm_{para\_Max}}} = 9.969 \cdot 10^{-1} \cdot (1 - RH)^{-2.220 \cdot 10^{-1}} \quad (11)$$

$$\frac{f(RH)_{637nm}}{f(RH)_{525nm_{para\_Max}}} = 9.951 \cdot 10^{-1} \cdot (1 - RH)^{-1.432 \cdot 10^{-1}} \quad (12)$$

and lower limits of:

$$\frac{f(RH)_{637nm}}{f(RH)_{457nm_{para\_Min}}} = 1.004 \cdot (1 - RH)^{7.785 \cdot 10^{-2}} \quad (13)$$

$$\frac{f(RH)_{637nm}}{f(RH)_{525nm_{para\_Min}}} = (1 - RH)^{5.145 \cdot 10^{-2}} \quad (14)$$

because:

$$f(RH)_{\lambda} = f(RH)_{637nm\_calc} / \frac{f(RH)_{637nm}}{f(RH)_{\lambda}}_{para} \quad (15)$$

From Eq. 1-2 and 15 the dry $\alpha_{sca}(\lambda)$ for the blue and green wavelengths can then be calculated as follows:

$$\alpha_{sca\_dry}(\lambda) = \alpha_{sca\_wet}(RH)_{\lambda} \cdot \frac{\alpha_{ext\_637nm}}{\alpha_{sca\_wet\_637nm}} \cdot \frac{f(RH)_{637nm}}{f(RH)_{\lambda}}_{para} \quad (16)$$

and using Eq. 11-14 the uncertainty on the dry $\alpha_{sca}(\lambda)$ can also be calculated.

$f(RH)_{637nm} / f(RH)_{\lambda}$ is close to unity, and deviate with increasing RH. Its uncertainty is a stronger function of the RH ranging from about ±9% (±5%) at RH=40% to about +45% and -27% (+23% and -21%) at RH=90% for the blue (green) wavelength.

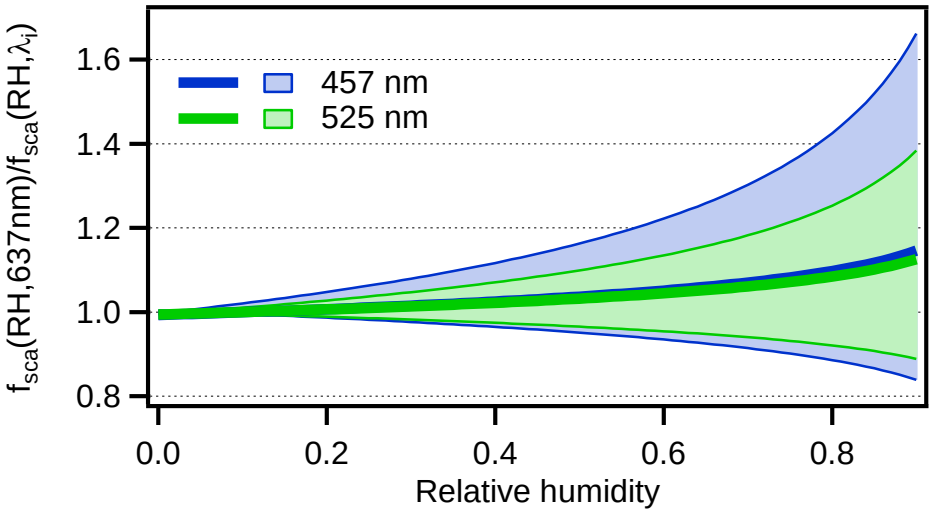

Figure S1: Ratio of the scattering enhancement factor of the red nephelometer wavelength ($f(RH)_{637nm}$) to the scattering enhancement factor of the blue and green nephelometer wavelengths ($f(RH,\lambda_i)$) as a function of RH. Bold lines are averaged values and shaded areas are an envelope of results for wide range parameter sweep of possible complex RI, κ and size distributions.

Additional figures

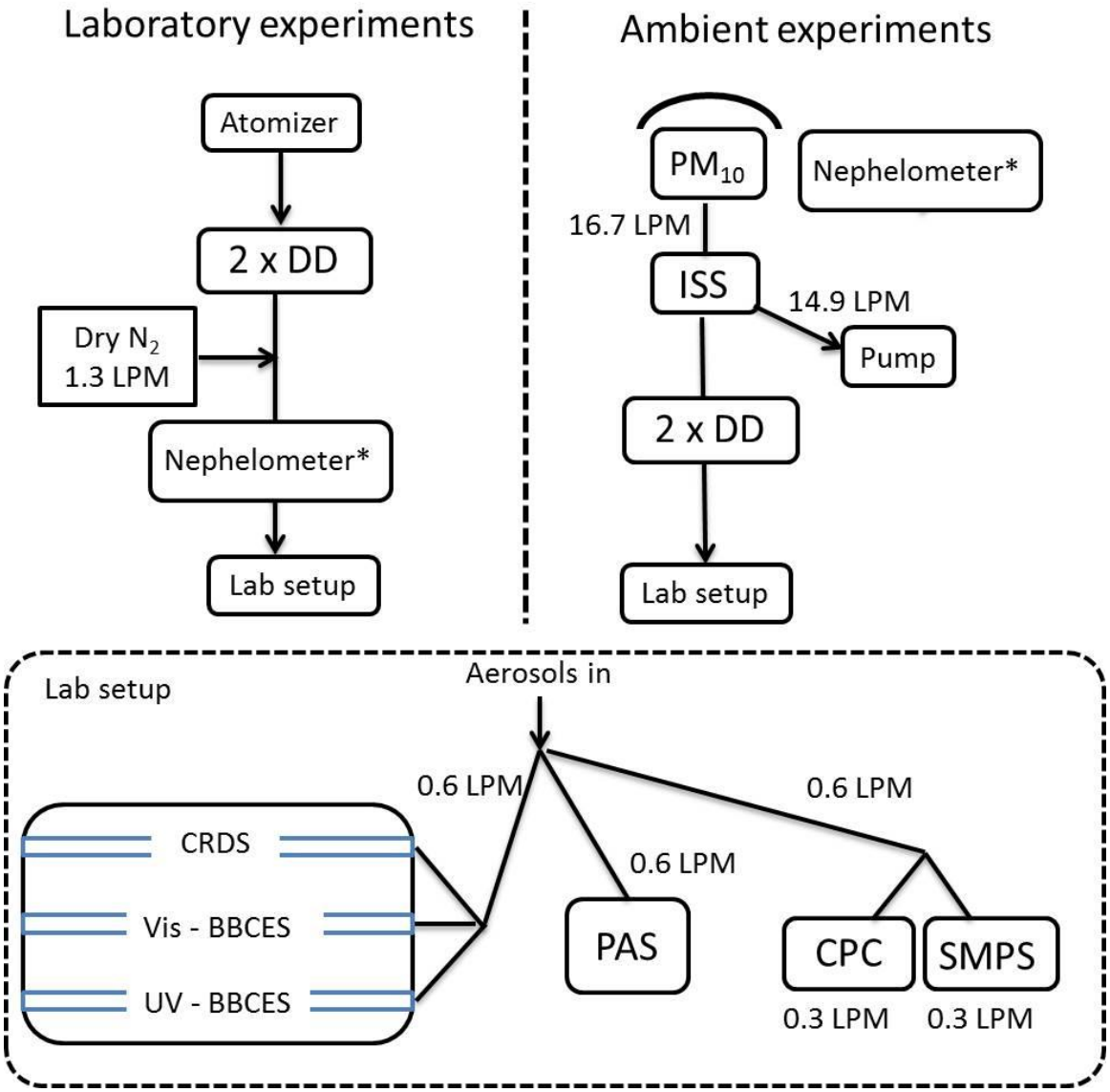

Figure S2. Left: schematic of the laboratory measurements. The nephelometer was position inside the laboratory and the aerosol went through it before being measured by the lab set up: optical system, PAS, CPC, and SMPS. Right: schematic of the ambient measurements. The nephelometer was moved and positioned on the roof. Abbreviations: DD, diffusion dryer; ISS, iso-kinetic splitter; CRD-S, cavity ring down spectrometer; BBCES, broadband cavity enhanced spectrometer; LPM, liter per minute; PAS, photoacoustic spectrometer; PM; particulate matter; CPC, condensation particle counter; SMPS, scanning mobility particle sizer.

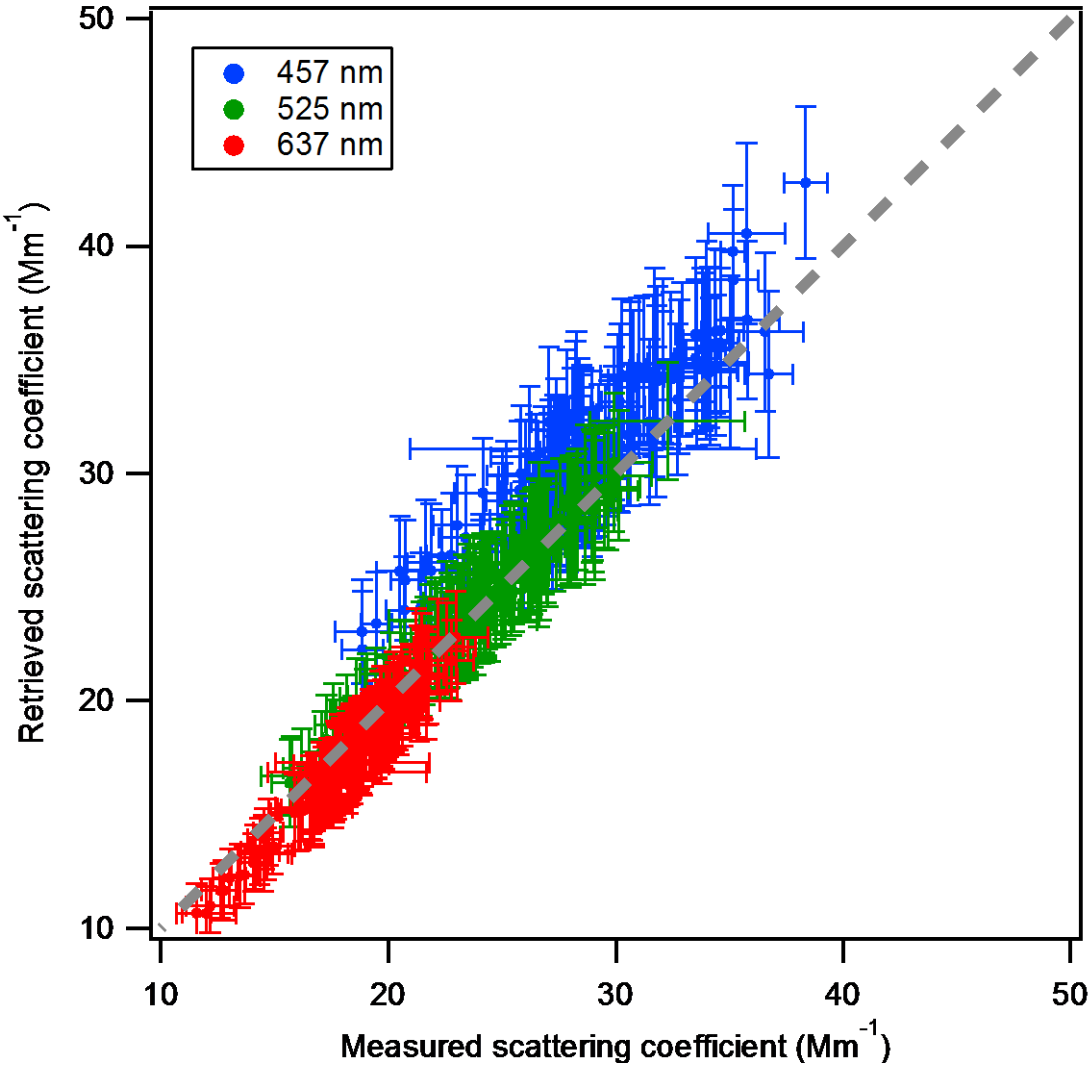

Figure S3. Retrieved and measured scattering coefficients at the nephelometer wavelengths (457, 525 and 637 nm).

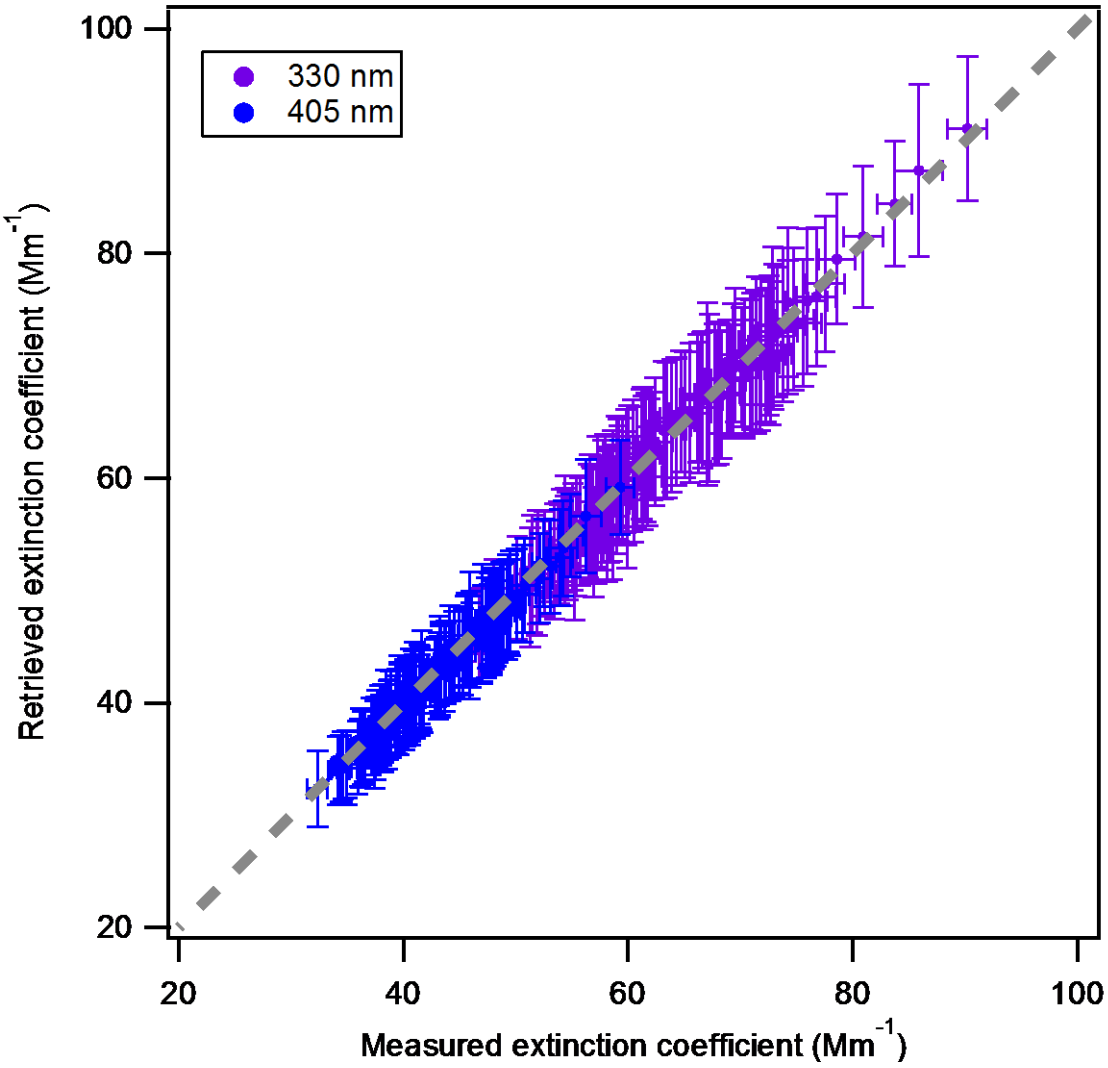

Figure S4. Retrieved and measured extinction coefficients at the center wavelengths of the two BBCES cavities (330 and 405 nm).

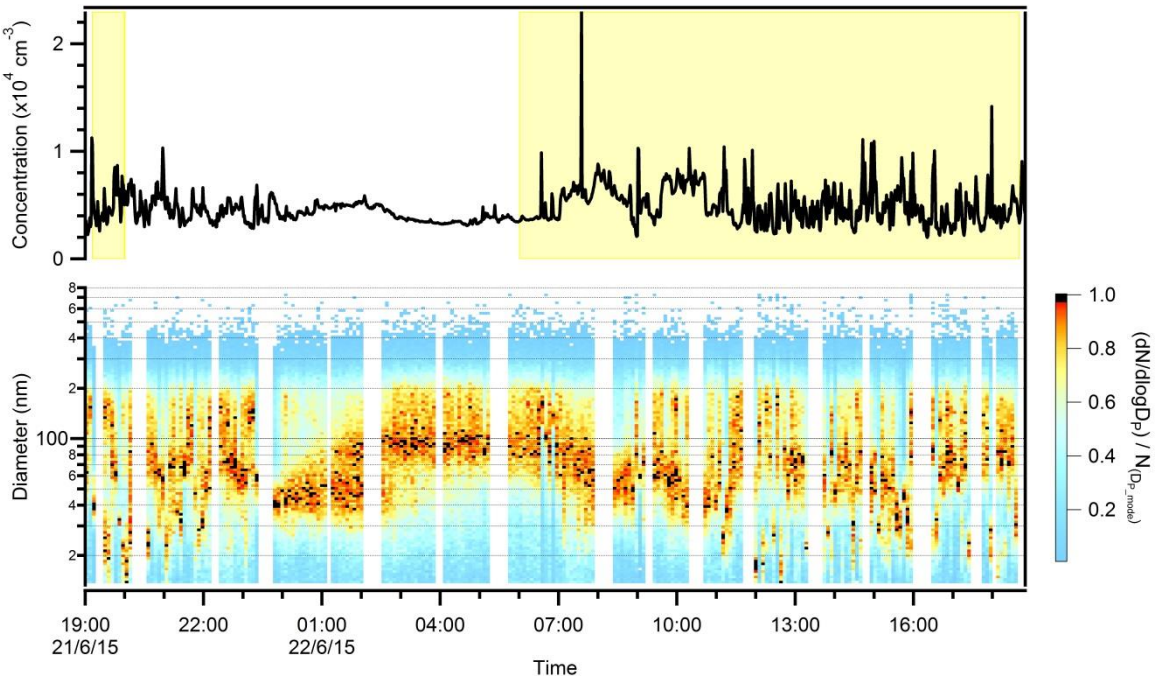

Figure S3. Time series of the total number concentration (N; upper panel) and of the size distributions obtained from the scanning mobility particle sizer normalized to the mode diameter concentration (lower panel).

References

Bohren, C. F., and Huffman, D. R.: Absorption and scattering of light by small particles, John Wiley & sons, INC, United States of America, 530 pp., 1983.

Flores, J. M., Bar-Or, R. Z., Bluvshtein, N., Abo-Riziq, A., Kostinski, A., Borrmann, S., Koren, I., Koren, I., and Rudich, Y.: Absorbing aerosols at high relative humidity: Linking hygroscopic growth to optical properties, Atmos. Chem. Phys., 12, 5511-5521, 2012.

Moise, T., Flores, J. M., and Rudich, Y.: Optical properties of secondary organic aerosols and their changes by chemical processes, Chemical reviews, 115, 4400-4439, 2015.

Nessler, R., Weingartner, E., and Baltensperger, U.: Adaptation of dry nephelometer measurements to ambient conditions at the jungfraujoch, Environ. Sci. Technol., 39, 2219-2228, 2005a.

Nessler, R., Weingartner, E., and Baltensperger, U.: Effect of humidity on aerosol light absorption and its implications for extinction and the single scattering albedo illustrated for a site in the lower free troposphere, 36, 958-972, 2005b.

Petters, M. D., and Kreidenweis, S. M.: A single parameter representation of hygroscopic growth and cloud condensation nucleus activity, Atmos. Chem. Phys., 7, 1961-1971, 2007.

Seinfeld, J. H., and Pandis, S. N.: Properties of the atmospheric aerosol, in: Atmospheric chemistry and physics: From air pollution to climate change, 2 ed., Wiley-Interscience, 350-389, 2006.

Snider, G., Weagle, C. L., Martin, R. V., van Donkelaar, A., Conrad, K., Cunningham, D., Gordon, C., Zwicker, M., Akoshile, C., Artaxo, P., Anh, N. X., Brook, J., Dong, J., Garland, R. M., Greenwald, R., Griffith, D., He, K., Holben, B. N., Kahn, R., Koren, I., Lagrosas, N., Lestari, P., Ma, Z., Martins, J. V., Quel, E. J., Rudich, Y., Salam, A., Tripathi, S. N., Yu, C., Zhang, Q., Zhang, Y., Brauer, M., Cohen, A., Gibson, M. D., and Liu, Y.: Spartan: A global network to evaluate and enhance satellite-based estimates of ground-level particulate matter for global health applications, Atmos Meas Tech, 8, 505-521, 2015.

Zieger, P., Fierz-Schmidhauser, R., Weingartner, E., and Baltensperger, U.: Effects of relative humidity on aerosol light scattering: Results from different european sites, Atmos. Chem. Phys., 13, 10609-10631, 2013.